Correlation of Quench Phenomena for Bottom Flooding during Loss-of-Coolant Accidents

Yoshio MURAO

*Japan Atomic Energy Research Institute**

Received November 18, 1977
Revised October 19, 1978

The three quench modes based on the observation with an outside-heated quartz tube experiment, *i.e.* (1) liquid column type, (2) dryout type and (3) droplet-rewetting type are discussed quantitatively to provide correlations for a reflood analysis code.

For the quench velocity of liquid column type and dryout type, using the data of PWR-FLECHT experiments, a correlation is obtained. This correlation is compared with experimental data and found that it can predict the inverse quench velocity within ±20% accuracy under the following conditions: pressure 1.0~4.1 kg/cm²·a, quench temperature 370~510°C, local subcooling 0~30°C, flow rate 5~25 cm/sec.

For the quench temperature of droplet-rewetting type, a correlation is derived and the prediction from it gives the qualitative agreement with few available data.

KEYWORDS: quench modes, liquid column type, dryout type, droplet-rewetting type, reflood analysis code, maximum liquid superheat, heat transfer, local liquid subcooling, PWR-FLECHT, quench velocity, quench temperature

I. INTRODUCTION

In order to develop a comptuer code for analysis on reflood process during postulated loss-of-coolant accidents, it is important to understand the quench phenomena.

Rewetting is essential for the establishment of normal and safe temperature levels of fuel rods. Rewetting is the re-establishment of liquid in contact with a hot surface of overheated fuel rods and the edge of the contact area, which is called a quench front, is advancing by progressive cooling of the surface. The advancing velocity is called a quench velocity (or rewetting velcoity) and the apparent temperature, at which a surface of fuel rods begins to be cooled rapidly and fallen down to nearly saturated temperature in a short time, is called a quench temperature. Experimental and theoretical studies on rewetting and quenching have been performed by many workers as reviewed by Butterworth & Owen[1].

Duffey & Pothouse[2] have analytically derived an approximate expression on the quench velocity from a two-dimensional heat conduction problem. It was assumed that:

(1) The water wets the surface up to the Leidenfrost temperature T_0 which is a constant with time and space.

(2) There is a constant heat transfer coefficient over all the wetted surface with a constant sink temperature, but no heat transfer over the dry surface. This approximation is based on the order of magnitude of the heat transfer coefficient for wetting ($\cong 10^4 W/m^2 \cdot °C$) compared to the one ($\cong 10^2 W/m^2 \cdot °C$) ahead of wetting.

(3) The two-dimensional Fourier equation of heat conduction is used

$$\frac{\partial^2 T}{\partial x^2}+\frac{\partial^2 T}{\partial y^2}=\frac{\gamma C}{\lambda}\cdot\frac{\partial T}{\partial t} \quad (1)$$

Obtained approximate solution for low rewetting rate ($Bi \equiv h\varepsilon/\lambda \ll 1$)

* *Tokai-mura, Ibaraki-ken.*

$$u^{-1}=\gamma C\left(\frac{\varepsilon}{h\lambda}\right)^{1/2}\frac{(T_w-T_s)^{1/2}(T_w-T_0)^{1/2}}{(T_0-T_s)}, \quad (2)$$

$$\cong\gamma C\left(\frac{\varepsilon}{h\lambda}\right)^{1/2}\frac{T_w-T_s}{T_0-T_s}, \quad (\text{for } T_0\cong T_s\ll T_w). \quad (3)$$

For high rewetting rate ($Bi\equiv h\varepsilon/\lambda\gg 1$)

$$u^{-1}\cong\frac{\pi\gamma C}{2h}\cdot\frac{T_w-T_s}{T_0-T_s}. \quad (4)$$

They concluded that the quench velocity is substantially independent of clad thickness and conductivity at high mass flows (>1.25 cm/sec: This value is calculated from the experimental condition of PWR-FLECHT[3].), and at lower mass flows, one-dimensional heat conduction model can be applied and the quench velocity is dependent on clad thickness and conductivity. Based on the one-dimensional heat conduction analysis, Yamanouchi[4] derived the same solution as Eq. (2). He determined the heat transfer coefficient h in Eq. (2) from his experiment on the quench with falling liquid film.

Recently, Blair[5] has derived the following equation with a consideration of all the terms in the series using an accurate asymptotic formula for the terms

$$u^{-1}=\frac{\pi}{2}\cdot\frac{\gamma C(T_w-T_0)}{h(T_0-T_s)}. \quad (5)$$

According to his explanation, the leading edge of the quenching front is a singular point in the mathematical solution and the singularity is evident from the slow convergence of the series expanded to both sides of the interface. Whereas Duffey & Porthouse have used the first term of the series.

In order to use the Eq. (5) practically, the determination of T_0 and h are necessary. The heat transfer coefficient h may be dependent on flow conditions. In practical coolant channel of a reactor core, heating power is enough to develop the two-phase flow and usually the flow pattern from single phase liquid flow to dispersed flow or superheated vapor flow can be observed. Therefore, the consideration of relation between quenching and flow pattern seems to be useful to understand the quench phenomena. So, we will discuss the flow patterns near the quench front and then consider a quench model.

II. Quench Model

1. Observation of Flow Pattern Near Quench Front

In the case of an actual fuel bundle, the coolant channel is surrounded with fuel rods and all surfaces around the coolant are considered to be high temperature during loss-of-coolant accidents. Under the above condition, the force applied to the water seems to be only gravitational force and frictional force with vapor at the two-phase interface.

To examine the flow pattern during reflood phase, from the bottom, the water was supplied into a transparent quartz tube heated outside[6]. Based on the flow patterns observed in the experiment, the quench modes are classified as shown in **Fig. 1** into the following three types:

(1) Liquid column type
(2) Dryout type (annular flow type)
(3) Droplet-rewetting type.

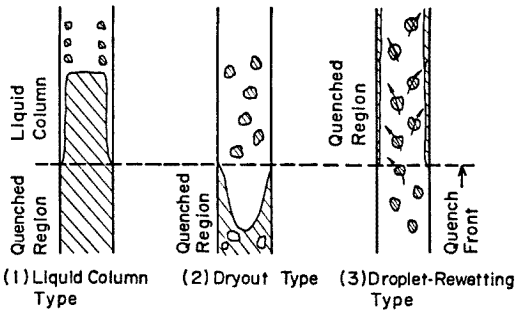

Fig. 1 Three types of quench mode

Type (1) is defined that the liquid column is formed downstream from quench front and the local temperature at the quench front is lower than saturation temperature.

Type (2) is defined that the two-phase flow exists at the quench front and the quench front can be considered to be dryout point. And usually the flow pattern is recognized as an annular flow at the quench front.

Type (3) appears at the low temperature

location and is considered to be resulted from wetting the wall with the water droplets.

In the quench of Types (1) and (2), the wall is wetted upstream from the quench front and the heat from unwetted part is released from the wetted wall. Therefore, the heat conduction model mentioned in Sec. II-1 seems to be available. The quench of Type (1) appears under the liquid subcooled condition at the quench front. The quench of Type (2) appears under the saturation condition of water at the quench front.

2. Maximum Liquid Superheat

Spiegler *et al.*[7] derived the maximum liquid superheat from the van der Waals' equation of state by using the assumption that the minimum pressure value in the P-V curve of the equation of state agrees with zero at the maximum temperature. His result is written as

$$T_M=27/32(T_{crit}+273.16)-273.16\,, \qquad (6)$$

where T_{crit} is a critical temperature. Of course, the assumption that the minimum pressure is zero is not correct. The pressure should be equal to the system pressure, but that makes difficult to derive the solution analytically.

Groeneveld[8] calculated numerically the maximum liquid superheat as a function of pressure and the result is plotted in **Fig. 2.**

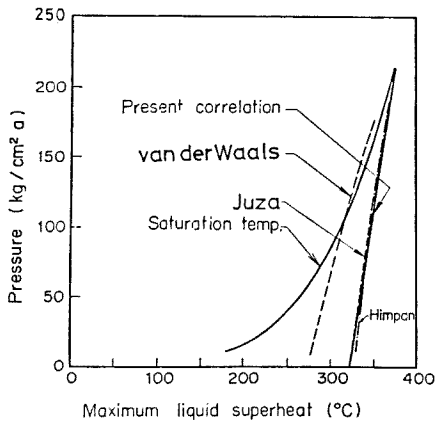

Fig. 2 Maximum liquid superheat[8] derived from Juza's, Himpan's and van der Waals' equation of state and present approximate correlation

To remove the obvious inconsistency that the maximum liquid superheat calculated from the van der Waals' equation of state is smaller than the saturation temperature at pressures above 100 kg/cm²·a, Groeneveld used Juza's equation of state and Himpan's one which are partly based on experimental data for water. These results are also plotted in Fig. 2. The present author made the following approximate correlation from Fig. 2:

$$T_M=321.05+0.237P\ (°C)\,, \qquad (7)$$

where P is a pressure (kg/cm²·a).

Another type of theoretical correlations is based on the nucleation rate in liquid. The liquid has some voids because the energy level of liquid is higher than that of solid and some positions which is considered to be filled with molecule in solid state are not occupied by molecule in liquid state. These are called a "hole". The probability of generation of holes enough to develop to nuclei of bubbles depends on the temperature. These theories give the temperature less than 270°C as a maximum superheat.

The maximum value measured in drop on hot plate experiment as a Leidenfrost temperature for stainless steel surface is 325°C[14] and the pulse heating experiment and capillary tube experiment indicate that the maximum superheat ranges from 270 to 300°C[15]. As indicated later, the inverse quench velocity has tendency to approach zero when the wall temperature of the quench front approaches about 320°C. That means that T_0 in Eq. (5) is about 320°C.

Therefore, Eq. (7) is adopted as a maximum liquid superheat for quench phenomena.

3. Dryout Type Quench

Based on the two-dimensional heat conduction model, the following simple model was adopted to explain the temperature distribution near the quenching region as shown in **Fig. 3.** In this figure, the hatched region 1 indicates the heat flow path from the width dx of quench front plane to the heat transfering surface and the region 2 indicates heat

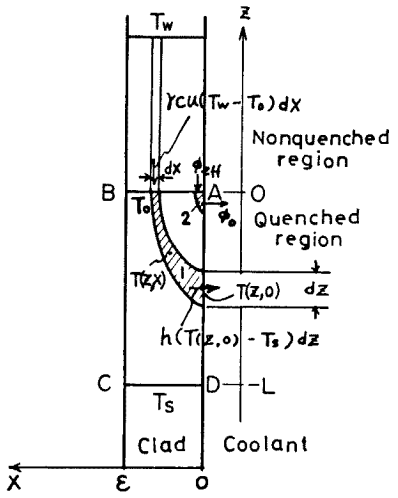

Fig. 3 Schematic illustration of two-dimensional heat conduction model

flow path near the quench front.

In this model, it was assumed that:

(1) The temperature distribution is one-dimensional in axial direction and there is no heat transfer over the surface which z is positive at $x=0$.

(2) The heat transfer coefficient h is constant over the wetted surface which z is negative.

(3) The opposite surface is adiabatic.

(4) The temperature approaches to T_w, when z approaches infinite, *i.e.* $\lim_{z\to\infty} T(z, x) = T_w$.

(5) At the quench front plane proceeding at a velocity u, the temperature equals T_0, *i.e.* $T(0, x)=T_0$, which is so-called the Leidenfrost temperature and at the temperature higher than it, water is considered to be impossible to be contact with heated wall.

(6) The coolant temperature is saturation temperature.

(7) The stored energy is completely released between $z=0$ and $-L$, that is, the wall temperature is saturation temperature at $z=-L$, *i.e.*

$$T(-L, x)=T_s .$$

Considering the heat balance in the region ABCD, the following equation is obtained

$$\int_0^{x=\varepsilon} \gamma C(T_w-T_0)u\,dx+\int_0^{x=\varepsilon} \gamma CSu\,dx = \int_{z=-L}^{0} h(T(z, 0)-T_s)dz$$

where $S=\int_0^x\int_{z-dz/2}^{z+dz/2}\frac{\partial T(z, x)}{\partial z}dz\,dx$, that is, S is a volumetric intergnal of temperature difference in axial direction over the volume of hatched region 1.

In left-hand side, the first and the second term indicates the heat release due to falling temperature from T_w to T_0 and from T_0 to $T(z, 0)$. The right-hand side term indicates the heat transfer to the coolant. When x, z approach zero, the considering element dx approach to quench front and the considering volume becomes the hatched region 2, that is, S becomes zero as a limit.

Making the limit of the above equation as x, z approach zero

$$\gamma C(T_w-T_0)u\,dx=h(T_0-T_s)dz .$$

Assuming that the $\lim_{dx,\,dz\to\infty}\left(\frac{dx}{dz}\right)=F_\phi$ and F_ϕ is a finite value,

$$u^{-1}=F_\phi\frac{\gamma C(T_w-T_0)}{h(T_0-T_s)} . \qquad (8)$$

Comparing Eq. (8) with Eq. (5) which is derived as an analytical asymptotic solution of the two-dimensional heat conduction problem, it can be considered that $F_\phi=\pi/2$ and the quench velocity is controlled only by the heat transfer near the quench front (point A in Fig. 3).

Assuming that the heat transfer mechanism is similar to boiling heat transfer, the heat flux is more meaningful than the heat transfer coefficient.

Therefore,

$$u^{-1}=F_\phi\frac{\gamma C(T_w-T_0)}{\phi_0}=\frac{\gamma C(T_w-T_0)}{\phi_{\text{eff}}} , \qquad (9)$$

where $\phi_0\equiv h(T_0-T_s)$

$$\phi_{\text{eff}}=\phi_0/F_\phi=(2/\pi)\phi_0 .$$

ϕ_0 and ϕ_{eff} mean the heat flux to the coolant and the axial heat flux at the quench front respectively. The heat flux ϕ_0 will be specified if ϕ_0 is a function of only liquid superheat,

$\Delta T_{sat}(\equiv T_0 - T_s)$, under the saturated condition.

In Fig. 3, we assumed that the water can wet the surface and surface heat flux is significantly high at the temperature equal to the liquid maximum superheat, *i.e.*

$$T_0 = T_M . \tag{10}$$

To determine the effective heat flux ϕ_{eff}, the inverse quench velocity calculated from the PWR-FLECHT data[3] by neglecting the release of the stored energy from heater rods are plotted against the quench temperature T_w as shown in **Fig. 4.**

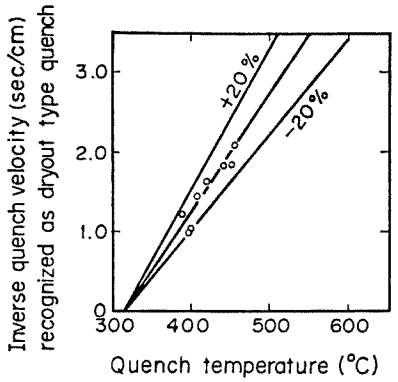

Fig. 4 Plot of inverse quench velocity against quench temperature using PWR-FLECHT data recognized as dryout type quench

From the figure, the best fit effective heat flux is determined as

$$\phi_{eff}/\gamma C = 2{,}363.3 \ (\mathrm{m}\cdot{}^\circ\mathrm{C/hr}) . \tag{11}$$

This correlation is presented in Fig. 4 by a solid line and the accuracy of it is within $\pm 20\%$. Considering that the clad material is stainless steel and γC is 927.10 kcal/m·°C,

$$\phi_{eff} = 2.19 \times 10^6 \ (\mathrm{kcal/m^2 \cdot hr}) , \tag{12}$$

$$\phi_0 = F_\phi \phi_{eff} = 3.44 \times 10^6 \ (\mathrm{kcal/m^2 \cdot hr}) . \tag{13}$$

Hence we can obtain the best fit correlation for quench velocity, *i.e.*

$$u^{-1} = \frac{\gamma C\{T_w - (321.05 + 0.237P)\}}{2.19 \times 10^6 \ (\mathrm{kcal/m^2 \cdot hr})} . \tag{14}$$

It is assumed that the "boiling curve" of the quench phenomena can be illustrated schematically in **Fig. 5** and the maximum heat flux ϕ_{MAX} corresponds to the heat flux ϕ_0, *i.e.*

$$\phi_{MAX} = 3.44 \times 10^6 \ (\mathrm{kcal/m^2 \cdot hr}) . \tag{15}$$

This assumption is based on the results of JAERI reflood experiment[9], that is, the boiling curves calculated from the temperature histories of clad surface during reflood phase have flat part after quench point. Because of the data averaging, the calculated heat flux is lower than the real heat flux.

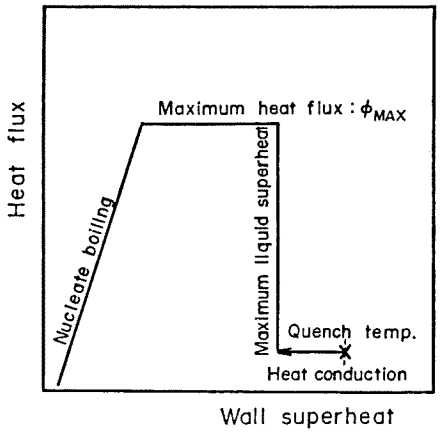

Fig. 5 Schematic diagram of heat flux *vs.* wall superheat

The temperature distribution of unwetted part which corresponds with the downstream from quench front can be calculated as follows, that is, as shown in **Fig. 6,** assuming that the heat flux from wall to coolant can be negligible, the heat conduction in axial direction is dominant and the heat flux at the quench front plane is ϕ_{eff}, the heat conduction

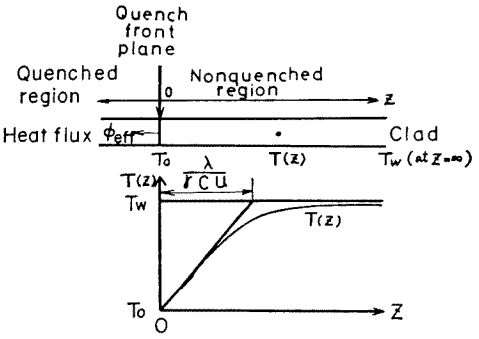

Fig. 6 Schematic diagram of axial temperature distribution in clad

equation is

$$\gamma C\frac{dT}{dt}+\lambda\frac{d^2T}{dz^2}=0. \tag{16}$$

The boundary conditions are as follows:

$$\left.\begin{aligned} &T=T_w \quad \text{at } z=\infty \\ &T=T_0 \quad \text{at } z=0 \\ &\lim_{z\to\infty}\frac{dT}{dz}=0 \\ &\phi_{\text{eff}}=\left(\lambda\frac{dT}{dz}\right)_{z=0} \end{aligned}\right\}. \tag{17}$$

Further assuming that the quench velocity is constant, *i.e.*

$$\frac{dz}{dt}=u. \tag{18}$$

Hence,

$$\gamma C\frac{dT}{dt}u+\lambda\frac{d^2T}{dz^2}=0. \tag{19}$$

Integrating the above equations with boundary conditions, the following equations are obtained:

$$T=T_w-(T_w-T_0)\exp\left(-\frac{\gamma Cuz}{\lambda}\right), \tag{20}$$

$$\phi_{\text{eff}}=(T_w-T_0)\gamma Cu. \tag{21}$$

The axial temperature distribution is schematically shown in Fig. 6 and is analogous to the temperature history of quenching on a point in axial direction. The distance and the period between the appearance of dominant temperature change and the initiation of wetting on the heat transfering surface can be approximately expressed as $\lambda/(\gamma Cu)$ and $\lambda/(\gamma Cu^2)$ respectively. For stainless steel, it is calculated that the thermal boundary thickness is 0.42 mm if the quench velocity is 1 cm/sec and the quench occurs in about 50 msec.

Practically, the quench occurs automatically in a short time when the wall temperature falls down to T_w, that is, from T_w to T_0 by axial heat conduction and below T_0 by excellent heat transfer of wetted region. Therefore, T_w can be considered as an "apparent quench temperature". As a measured quench temperature is usually more than 370°C, the temperature drop down to saturation temperature is more than 200°C. Therefore, the error of 20°C in estimating the terminal temperature after quenching is less than 10% error of the stored energy released during quenching. So that error is practically allowable even if the ordinal nucleate boiling correlation is adopted as a nucleate boiling after quenching. Based on the above-mentioned reason, the boiling curve as shown in Fig. 5 is adopted.

4. Liquid Column Type Quench

The quench mode of this type occurs under the subcooled condition at the quench front. As the critical heat flux of boiling is a function of liquid subcooling, the heat flux to coolant at the quench front ϕ_0 is assumed to be a function of liquid subcooling and to be simplified as a function of the following form,

$$\phi_0=\phi_{0\,sat}(1+a\Delta T_{sub}{}^n), \tag{22}$$

where $\phi_{0\,sat}$ is a heat flux to coolant at the quench front with no liquid subcooling, ΔT_{sub} a liquid subcooling, and a and n constants. It is further assumed that the effective heat flux becomes the heat flux of dryout type quench as the liquid subcooling decrease to zero at the quench front, *i.e.* from Eq. (12) the best fit form can be written as

$$\phi_{0\,sat}=2.19\times10^6\ (\text{kcal/m}^2\cdot\text{hr}).$$

Hence the inverse quench velocity of the best fit form can be written as

$$u^{-1}_{\text{liquid column}}=\frac{\gamma C\{T_w-(321.05+0.237P)\}}{2.19\times10^6(1+a\Delta T_{tub}{}^n)}$$

$$=\frac{u^{-1}_{\text{dryout}}}{1+a\Delta T_{sub}{}^n}. \tag{23}$$

Now we introduce the parameter X defined as

$$X=\frac{u_{\text{liquid column}}}{u_{\text{dryout}}}-1=a\Delta T_{sub}{}^n. \tag{24}$$

Using the data from PWR-FLECHT[3], X and ΔT_{sub} are plotted in **Fig. 7.** The two coefficients a and n are determined as follows:

$$a=2.778\times10^{-5}$$
$$n=3. \tag{25}$$

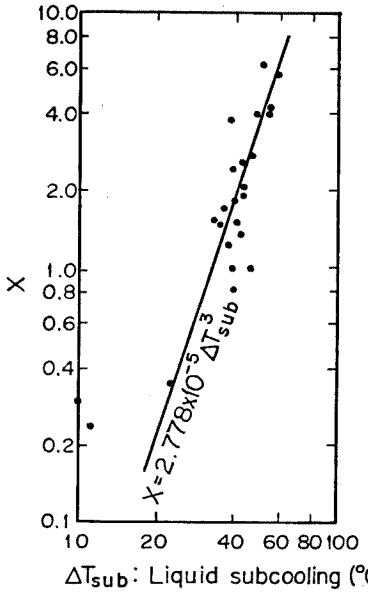

Fig. 7 Plot of X defined by Eq. (24) against liquid subcooling (Data source is PWR-FLECHT.)

The following correlations can be obtained from above discussion.

$$u^{-1}=\frac{\gamma C\{T_w-(321.05+0.237P)\}}{2.19\times10^6(\text{kcal/m}^2\cdot\text{hr})(1+2.778\times10^{-5}\Delta T_{sub}{}^3)}. \tag{26}$$

The maximum heat flux is

$$\phi_0=3.44\times10^6(1+2.778\times10^{-5}\Delta T_{sub}{}^3)\ (\text{kcal/m}^2\cdot\text{hr}). \tag{27}$$

There correlations can be available even in the case of dryout type quench.

5. Droplet-rewetting Type Quench

The upper limit temperature which the water can wet the heated wall is considered to be the maximum liquid superheat T_M which is derived as Eq. (7), *i.e.*

$$T_M=321.05+0.237P\ (^\circ\text{C}).$$

When very little water comes to the heated wall, the temperature drop due to contact of the water with the wall is considered to be nearly zero and the quench temperature is nearly equal to the liquid maximum superheat, *i.e.*

$$T_Q\cong T_M. \tag{28}$$

But when much water comes to the heated wall, the temperature of the heating wall surface decreases to the so-called contact temperature[12] which is derived with the assumption that the temperature dependence of the physical properties can be negligible and defined as

$$T_{cont}=\frac{T_l\sqrt{(\lambda\gamma C_P)_l}+T_c\sqrt{(\lambda\gamma C)_c}}{\sqrt{(\lambda\gamma C_P)_l}+\sqrt{(\lambda\gamma C)_c}}. \tag{29}$$

If the contact temperature is equal to or lower than the maximum liquid superheat, *i.e.*

$$T_M\geqq T_{cont}, \tag{30}$$

the water can exist on the heated wall, that is, the water can wet heated wall. The maximum wall temperature, at which the water can wet the heated wall, can be defined as a quench temperature of droplet-rewetting type quench and the temperature can be obtained with $T_{cont}=T_M$ as

$$T_Q=T_M+K(T_M-T_l), \tag{31}$$

where

$$K=(\lambda_l\gamma_l C_{Pl})^{1/2}/(\lambda_c\gamma_c C_c)^{1/2}. \tag{32}$$

Generally, the factor K can be written as

$$K=A(\lambda\gamma C_P)^{1/2}/(\lambda_c\gamma_c C_c)^{1/2}, \tag{33}$$

where A is a factor to consider the collision rate of the water droplets to the heated wall, *e.g.* A is unity when the void fraction is 0 and A is zero when the void fraction is nearly 1.

For stainless steel as a heated wall material, assuming that the water is at the saturation temperature, then $K=0.1895$, from Eq. (33) and

$$T_{Q.A=1}=363.5(^\circ\text{C})\ (\text{at } 1\ \text{kg/cm}^2\cdot\text{a})$$
$$=355.8(^\circ\text{C})\ (\text{at } 4\ \text{kg/cm}^2\cdot\text{a})$$
$$T_{Q.A=0}=321.5(^\circ\text{C}).$$

For Zircaloy 2, then $K=0.3210$ and

$T_{Q.A=1}=392.3(°C)$ (at 1 kg/cm²·a)
$=378.2(°C)$ (at 4 kg/cm²·a),
$T_{Q.A=0}=321.5(°C)$.

III. DISCUSSION

1. Quench Characteristics Appeared in PWR-FLECHT Data

In **Fig. 8,** the quench temperatures of heater rod named 5F in PWR-FLECHT experiment[3] are plotted against the time ratio, which is defined as the ratio of the quench time to the apparent arrival time of the water. Most of the quench temperatures are in the range of 320~510°C. The symbol X indicates the data that the quench occurs earlier at the position of the top thermocouple than at the one of the second top thermocouple. Therefore, the quench symboled X may be considered as the droplet-rewetting type quench. The data symboled A is a special data which is taken at the high flooding velocity, *i.e.* 44.7 cm/sec. The region which the time ratio is nearly unity means the fast quench and it can be considered to be quench due to wetting wall surface rapidly with considerable amount of water which has been pushed by vapor generated upstream of test section.

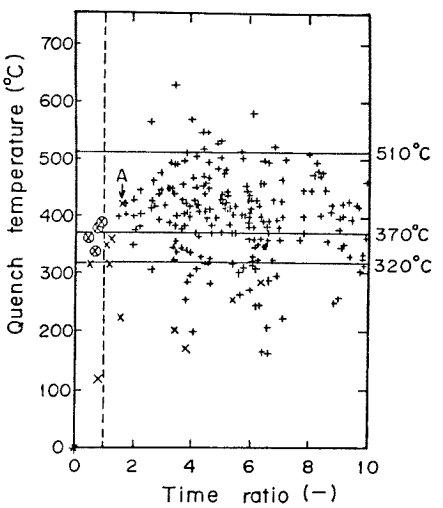

Fig. 8 Plot of quench temperature against time ratio (Time ratio is defined as a ratio of quench time to apparent arrival time of water.)

The symbol ⊗ indicates the data taken under the same criteria but measured under nearly atmospheric pressure. The most of the data symboled X are measured under a pressure of 4 kg/cm²·a. Except A, the quench temperatures of the data symboled X are lower than 360°C, which is about the same quench temperature of droplet-rewetting type 355.8°C for stainless steel under 4 kg/cm²·a. For stainless steel under atmospheric pressure, such a quench temperature is 363.5°C. However the measured quench temperatures (symboled ⊗) are ranging from 340 to 385°C and the value is slightly higher than the predicted value.

Roughly speaking, the quench temperature of droplet-rewetting type is agree with the one of PWR-FLECHT data qualitatively. But to confirm the assumption, much more data are necessary.

2. Comparison of Present Correlation with Thompson's Correlation

Thompson[10] has derived the following empirical correlation from his experimental data and Blair's analysis[6]

$$u^{-1}=\frac{\gamma C\{T_w-(327+\Delta T_{sub})\}}{1.84\times10^6(\text{kcal/m}^2\cdot\text{hr})}. \tag{34}$$

When the liquid subcooling equals zero, *i.e.* $\Delta T_{sub}=0$, the Thompson's correlation is nearly same as our correlation. The main difference in both correlations exists in treatment of the liquid subcooling. To check the reliability on these correlations, the quench velocities calculated from both correlations were compared with the quench velocities based on the PWR-FLECHT Group 1 data[3]. The results are shown in **Fig. 9**(a) and (b).

Our correlation is considered to be more reliable than Thompson's correlations.

We should note the fact that the coefficients of the present correlation have been determined from the PWR-FLECHT data themselves.

3. Check of Present Correlations using Piggott-Porthouse's Data

Piggott & Porthouse[11] carried out the

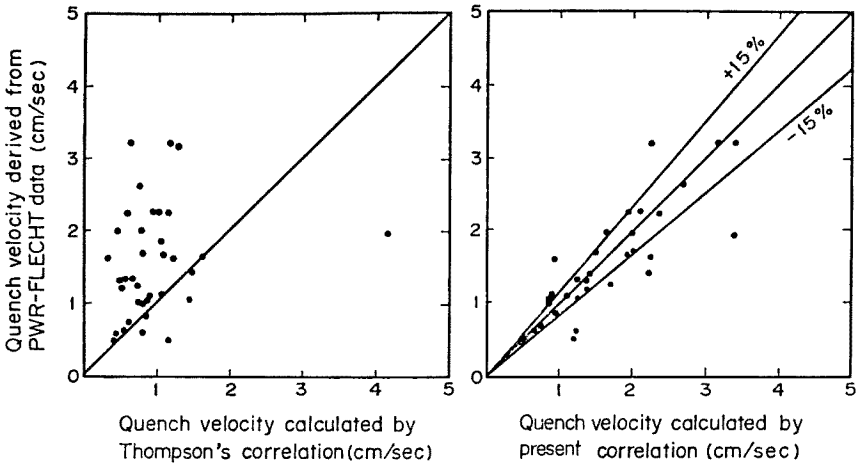

(a) Thompson's correlation (b) Present correlation

Fig. 9 Comparison of quench velocity calculated by Thompson's and present correlations with PWR-FLECHT data

bottom flood experiment using annulus test section. An Inconel-clad, magnesium oxide-filled heater rod (1.27 cm dia., 0.085 cm clad thickness, 20 cm heated length) was mounted concentrically within a 2.5 cm bore Pyrex tube and water was supplied from a constanthead tank. The time for the rewetting front to traverse between two marks 10 cm apart was measured with a stopwatch. They plotted the inverse rewetting rate against the product of flow rate and inlet subcooling as shown in **Fig. 10**.

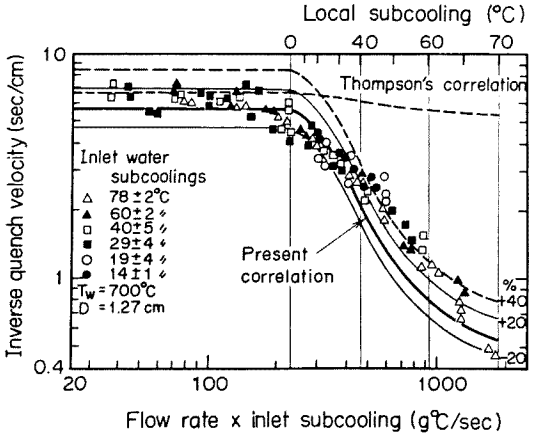

Fig. 10 Comparison of calculated quench velocity with Piggott-Porthouse's data

Referring to the Fig. 3 of their paper[11] and the description that the water was saturated at flow rate 3 g/sec for 80°C inlet subcooling, the local subcooling can be determined as shown in top of Fig. 10. Then we plotted two correlations, *i.e.* Thompson's correlation Eq. (34) and our correlation Eq. (26) on the Fig. 10. It was found that our correlation gave fairly good agreement with measured results.

4. Discussion on "Boiling Curve" of Quench Phenomena

The "boiling curve" of quench phenomena is presented in Fig. 5 as a schematic diagram of heat flux *vs.* wall superheat. This diagram is different from usual boiling curves, that is, our boiling curve has not so-called transition boiling region. Tachibana & Enya[13] plotted the "boiling curve" in quench of solid copper cylinder (8 mm dia., 70 mm long) in water. The boiling curves has a transition boiling region. The difference is considered to be attributed to the difference of the heat conductivity and the stored energy which determine the vapor generation history during the quenching.

In the case of fuel-simulated heater rods or nuclear fuel rods discussed in this paper, the sufficient heat is not supplied from inner part in quenching due to small heat capacity of clad and low heat conductivity of internal material. Therefore, the temperature of clad

surface falls down to nucleate boiling temperature in a short time without enough formation of vapor film layer on the clad surface to establish the stable film or transition boiling.

5. Reliability Range of Correlations

The quench velocity correlation is based on the PWR-FLECHT Group 1 data to determine the constants of it. The data were taken under the condition ranging 1.1 to 4.1 kg/cm²·a in the system pressure, 370 to 510°C in the quench temperature, 0 to 60°C in the local subcooling and 5 to 25 cm/sec in the flow rate. Most of the data can be correlated with the equation within ±15% accuracy.

The Piggott & Porthouse's data were taken at the atmospheric pressure, the initial wall temperature (it is considered to be nearly same as the quench temperature) of 700°C and the local subcooling ranged from 0 to 70°C. Their data taken under the condition ranging 0 to 30°C in the local subcooling agree with the curve predicted by the equation within ±20% accuracy, but for the data of higher subcooling, the agreement is not so good, that is, the accuracy is within 0 to ±40%.

Therefore, the equation is considered to predict the inverse quench velocity within ±20% accuracy under the condition ranging 1.0 to 4.1 kg/cm²·a in the pressure, 370 to 510°C in the quench temperature, 0 to 30°C in the local subcooling and 5 to 25 cm/sec in the flow rate.

IV. Conclusions

(1) The three quench modes based on the observation with an outside-heated quartz tube experiment[6], *i.e.* (a) liquid column type, (b) dryout type and (c) droplet-rewetting type, are discussed quantitatively to provide correlations for a reflood analysis code.

(2) For quench velocity of the liquid column type and the dryout type, using the data of PWR-FLECHT experiments[3], the following correlation is obtained

$$u^{-1}=\frac{\gamma C\{T_w-(321.05+0.237P)\}}{2.19\times10^6(\mathrm{kcal/m^2\cdot hr})(1+2.778\times10^{-5}\Delta T_{sub}{}^3)}.$$

This correlation is compared with the data of PWR-FLECHT Group 1 experiments[3] and the Piggott & Porthouse's experiments[11] and it is found that it can predict the inverse quench velocity within ±20% accuracy under the following conditions:

Pressure: 1.0~4.1 kg/cm²·a
Quench temperature: 370~510°C
Local subcooling: 0~30°C
Flow rate: 5~25 cm/sec.

(3) For the quench of the droplet-rewetting type, the quench temperature is derived as

$$T_Q=T_M+K(T_M-T_l),$$

where T_M is defined in Eq. (7),

$$K=A(\lambda_l\gamma_l C_{Pl})^{1/2}/(\lambda_c\gamma_c C_c)^{1/2}$$

and A is constant for expressing flow condition ($A=1$ for $\alpha=0$, $A=0$ for $\alpha\cong1$, where α is void fraction). For some FLECHT-Group 1 data regarded as the quench of the droplet-rewetting type, the prediction with $A=1\sim0$ gives the qualitative agreement with the data. But to confirm this model and determine the expression of the factor A, much more data are necessary.

[Nomenclature]

A: Factor for collision rate of water droplets in Eq. (33)
a: Constant in Eq. (22)
B_i: Biot number ($\equiv h\ \varepsilon/\lambda$)
C, C_P: Specific heat (kcal/kg·°C)
F_ϕ: Factor defined in Eq. (8)
h: Heat transfer coefficient (kcal/m²·hr·°C)
n: Constant in Eq. (22)
P: System pressure (kg/cm²·a)
T: Temperature (°C)
T_{cont}: Contact temperature defined in Eq. (29)
T_M: Maximum liquid superheat
T_0: Temperature at quench front (Leidenfrost temperature)
T_Q: Quench temperature (°C)
T_S: Saturation temperature (°C)
T_W: Wall temperature just before quench (apparent quench temperature) (°C)

t: Time (hr)
u: Quench velocity (m/hr)
X: Factor defined in Eq. (24)
K: Factor defined in Eq. (32) or (33)
x: Co-ordinate in thickness direction (m)
y: Axial distance from arbitrary reference point (m)
z: Axial distance from quench front (m)
α: Void fraction
γ: Specific weight (kg/m^3)
ΔT_{sub}: Liquid subcooling (°C)
ε: Thickness of slab (m)
ϕ: Heat flux (kcal/m^2·hr)
ϕ_0: Heat flux to coolant at quench front (kcal/m^2·hr)
ϕ_{0sat}: Heat flux ϕ_0 with no liquid subcooling (kcal/m^2·hr)
ϕ_{eff}: Effective heat flux in axial direction at quench front (kcal/m^2·hr)
ϕ_{MAX}: Maximum heat flux described in Fig. 5 (kcal/m^2·hr)
λ: Heat conductivity (kcal/m^2·hr)

Subscripts

c: Wall (clad surface), l: Liquid
Liquid column: For liquid column type quench
Dryout: For dryout type quench

Physical properties used in this paper

Water
C_P=1 kcal/kg°C, γ=1,000 kg/m^3
λ=0.586 kcal/m·hr·°C

Stainless steel
C=0.118 kcal/kg·°C, γ=7,860 kg/m^3
λ=17.6 kcal/m·hr·°C

Zircaloy 2
C=0.0789 kcal/kg·°C, γ=6,570 kg/m^3
λ=10.97 kcal/m·hr·°C

Saturation temperature of water
At 1 kg/cm^2·a: 100°C
At 4 kg/cm^2·a: 143.6°C

ACKNOWLEDGMENT

The author is deeply indebted to Mr. T. Sudoh for his help in the calculation of the local subcooling from FLECHT Group 1 data and in the outside-heated quartz tube experiment.

The author is also grateful to Dr. M. Nozawa and Dr. K. Hirano of the Japan Atomic Energy Research Institute for helpful suggestions.

REFERENCES

(1) BUTTERWORTH, K., OWEN, R.G.: The quenching of hot surfaces by top and bottom flooding (Review), *AERE-R*-7992, (1975).
(2) DUFFEY, R.B., PORTHOUSE, D.T.C.: The physics of rewetting in water reactor emergency core cooling, *Nucl. Eng. Design*, **25**, 379～394 (1973).
(3) CERMAK, J.O., *et al.*: PWR full length emergency cooling heat transfer (FLECHT) Group 1 test report, *WCAP*-7435, (1970).
(4) YAMANOUCHI, A.: Effect of core spray cooling in transient state after loss of coolant accident, *J. Nucl. Sci. Technol.*, **5**[11], 547 (1968).
(5) BLAIR, J.M.: An analytical solution to a two-dimensional model of the rewetting of a hot dry rod, *Nucl. Eng. Design*, **32**, 159～170 (1975).
(6) MURAO, Y., SUDOH, T.: A study on quench phenomena during reflood phase (1. Quench models for bottom flooding), *JAERI-M* 6984, (1977).
(7) SPIEGLER, P., *et al.*: Onset of stable film boiling and the foam limit, *Int. J. Heat Mass Transfer*, **6**, 987～994 (1963).
(8) GROENEVELD, D.C.: The thermal behaviour of a heated surface at and beyond dryout, *AECL* -4309, (1972).
(9) MURAO, Y., *et al.*: Report on reflood series 1 Experiment, *JAERI-M* 6551, (in Japanese), (1976).
(10) THOMPSON, T.S.: Rewetting of a hot surface, *AECL*-5060, (1975). (Reprint of Paper B3.13 presented at the 5th Int. Heat Transfer Conf. Tokyo, Sep. 3～7, 1974.)
(11) PIGGOTT, B.D.G., PORTHOUSE, D.T.C.: A correlation of rewetting data, *Nucl. Eng. Design*, **32**, 171～181 (1975).
(12) For example,
ECKERT, E.R.G., DRAKE, R.M.: *"Analysis of Heat and Mass Transfer"*, (1972), McGraw-Hill;
MYERS, G.E.: *"Analytical Methods in Conduction Heat Transfer"*, (1971), McGraw-Hill.
(13) TACHIBANA, F., ENYA, S.: Heat transfer problems in quenching, *Bull. JSME*, **16**[91], 100～109 (1973).
(14) BAUMEISTER, K.J., *et al.*: Role of the surface in the measurements of the Leidenfrost temperature, *"Augmentation of Convective Heat and Mass Transfer"*, 91～101 (1970), ASME.
(15) COLE, R.: *"Boiling Nucleation, Advances in Heat Transfer"*, Vol. 10, 85～166 (1974), Academic Press.